

## Determination of the Intensities of Low- $Z$ Components of the Primary Cosmic Radiation at $\lambda = 41^\circ$ Using a Čerenkov Detector\*

WILLIAM R. WEBBER AND FRANK B. McDONALD  
*Department of Physics, State University of Iowa, Iowa City, Iowa*

(Received July 5, 1955)

A measurement of the intensities of the low- $Z$  components of the primary cosmic radiation has been made in the upper atmosphere at a depth of 13 g/cm<sup>2</sup> by means of a "Skyhook" balloon flown at  $\lambda = 41.5^\circ$ . The measuring instrument consisted of a thin (3.0 g/cm<sup>2</sup>) Čerenkov detector placed within the solid angle of a Geiger counter telescope. A Čerenkov detector was used because of its unique discrimination against slow particles. A system of guard and shower counters and circuits was included to identify side showers and background events occurring in the detector. A vertical intensity of  $82 \pm 9$  alpha particles/meter<sup>2</sup> steradian sec, at the top of the atmosphere was obtained, based on 374 counts attributed to alpha particles. Data obtained as the balloon rose to altitude gave a value of  $43 \pm 8$  g/cm<sup>2</sup> for the apparent absorption mean free path of alpha particles in air. An upper limit was set on the intensity of primary protons at this depth. In addition, a small number of counts that could be attributed to particles with  $3 \leq Z \leq 5$  were obtained and are discussed.

### I. INTRODUCTION TO THE PROBLEM

IT is now well known that the primary cosmic radiation consists of atomic nuclei stripped of their orbital electrons. The nuclei of hydrogen and helium (protons and alpha particles) predominate, with heavier nuclei up to iron occurring in lesser number. Ultimately one would like to know the intensity and energy spectrum of each of these components, as this information should be of great help in understanding the origin of the cosmic radiation and its propagation to the earth.

Previous experimenters have used ionization chambers,<sup>1,2</sup> proportional counters,<sup>3</sup> scintillation counters<sup>4,5</sup> and photographic emulsions<sup>6,7</sup> to analyze the composition of cosmic radiation at or near the top of the atmosphere. Each of the above methods has certain disadvantages which limit its effectiveness in the measurement of the intensity of heavy primaries at balloon altitudes. The foremost disadvantage of all the above methods is that low-energy singly charged secondaries (which indeed are very numerous at balloon altitudes) are often indistinguishable from high-energy multiply charged particles.

A Čerenkov detector makes possible an essentially new attack on this problem. The output from a Čerenkov detector (in the form of electromagnetic radiation—some of which is in the optical spectral region) due to the passage of a particle with charge  $Ze$  and velocity  $\beta c$  is given by

$$N = \frac{2\pi Z^2 l}{137} \left[ \frac{1}{\lambda_1} - \frac{1}{\lambda_2} \right] \left( 1 - \frac{1}{\beta^2 n^2} \right), \quad (1)$$

\* Assisted by joint program of the Office of Naval Research and the U. S. Atomic Energy Commission.

<sup>1</sup> Ellis, Gottlieb, and Van Allen, Phys. Rev. **95**, 147 (1954).

<sup>2</sup> G. W. McClure, Phys. Rev. **96**, 1391 (1954).

<sup>3</sup> G. J. Perlow *et al.*, Phys. Rev. **88**, 321 (1953).

<sup>4</sup> E. P. Ney and D. M. Thon, Phys. Rev. **81**, 1069 (1951).

<sup>5</sup> L. Bohl, Ph.D. thesis, University of Minnesota, 1954 (unpublished).

<sup>6</sup> H. Bradt and B. Peters, Phys. Rev. **77**, 54 (1950).

<sup>7</sup> Kaplon, Noon, and Racette, Phys. Rev. **96**, 1408 (1954).

where  $N$  = number of quanta emitted between wavelengths  $\lambda_1$  and  $\lambda_2$ ,  $n$  is the index of refraction of the medium, and  $l$  is the path length of the particle in the medium.

A plot of  $N/Z^2$  vs  $\beta$  for various particles is shown in Fig. 1.

The most important features of Eq. (1) are:

(a) The output is proportional to  $Z^2$ . Thus, like ionization detectors the Čerenkov detector has the basic characteristics for  $Z^2$  discrimination among the particles passing through it.

(b) A Čerenkov output occurs only when a charged particle passes through the medium with a velocity greater than  $c/n$ . For Lucite this threshold velocity corresponds to  $\beta = 0.67$ ; thus this apparatus is insensi-

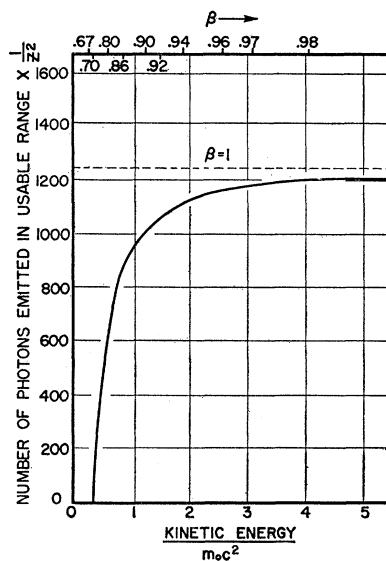


FIG. 1. Number of Čerenkov photons emitted as a function of the energy for particles with constant velocity. (Curves are for this particular apparatus —  $l = 2.59$  cm,  $\lambda_1 = 3000$  Å,  $\lambda_2 = 7000$  Å,  $n = 1.50$ .)

tive to many of the low-energy secondaries that plague other experimenters.

(c) Last and most important: The size of the output from a Čerenkov detector diminishes as  $\beta$  becomes smaller. This is in distinct contrast to the behavior of an ionization detector in which the output varies approximately as  $1/\beta^2$ . Thus low-energy singly charged secondaries give outputs *smaller* than high-energy singly charged particles and make little or no contribution in the range of outputs characterizing high-energy particles having  $Z \geq 2$ .

Pioneering investigations of cosmic radiation at high altitudes using Čerenkov detectors have been made by the Minnesota group which has used the directional properties of the radiation to study the albedo problem.<sup>8</sup> More recent measurements of the low-Z components of the primary radiation using this type of detector have also been made by this group.<sup>9,10</sup> The Iowa work confirms and extends the Minnesota experiments in the determination of improved values of absolute intensities of the cosmic-ray primaries of low Z. Results of a successful balloon flight at  $\lambda=41.5^\circ$  are reported herein. In addition, there is now being undertaken here at Iowa an extensive survey of the primary radiation at lower latitudes using Čerenkov detectors and at higher latitudes using a combination of a Čerenkov detector and scintillation counter.

II. DESCRIPTION AND OPERATION OF THE EQUIPMENT

The apparatus comprised the following main sections:

(1) Čerenkov detector.—The Čerenkov detector consisted of a Lucite block optically coupled to a photomultiplier tube (Fig. 2).

(2) Geiger counter telescope.—The Čerenkov detector was placed between the two trays of a Geiger counter telescope whose axis was vertical. The geometric factor

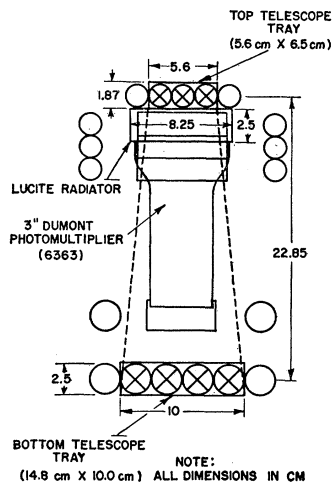


FIG. 2. Outline drawing of Geiger counter telescope and Čerenkov detector showing arrangement of guard and shower counters. Telescope counters designated  $\otimes$ ; guard counters  $\circ$ .

<sup>8</sup> J. Winckler and K. Anderson, Phys. Rev. **93**, 596 (1954).

<sup>9</sup> N. Horowitz, Phys. Rev. **98**, 165 (1955).

<sup>10</sup> J. Linsley, Phys. Rev. **97**, 1292 (1955).

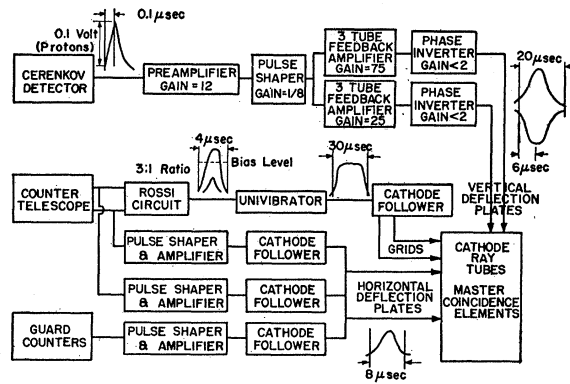


FIG. 3. Block diagram of the equipment.

of the telescope was determined by calculation, using measured effective lengths of the individual counters.<sup>11</sup> For an isotropic flux it was  $9.27 \pm 0.5$  steradian  $\text{cm}^2$ .

(3) Guard and shower system.—The guard counters were arranged according to Fig. 2. The electronic circuitry was such that if a particle passed through any of the guard counters simultaneously with a telescope coincidence the corresponding Čerenkov output pulse was “marked.”

Shower detection was accomplished in the following manner: If two or more counters in either the bottom or the top tray were triggered simultaneously the associated circuitry was such that the corresponding Čerenkov output pulse was “marked” in a manner similar to that for a guard count.

(4) Electronics.—A block diagram of the electronics is shown in Fig. 3. The main features of the various sections are as follows:

(a) Čerenkov pulse amplifiers. The pulses from the photomultiplier were amplified by a pair of 4 tube “pulse shaping” feedback amplifiers.<sup>12</sup> These amplifiers were linear throughout 90% of their range and had characteristics which were insensitive to voltage change. Pulses from particles with  $Z \leq 2$  appeared in the linear region on the CRT (cathode-ray tube) attached to the high-gain amplifier while those pulses from particles with  $Z \leq 5$  appeared in the linear region on the CRT attached to the low-gain amplifier.

(b) Coincidence and intensifier circuits. The purpose of these circuits was to apply a “gating” pulse to the grids of the CRT whenever a particle passed through the telescope. This gating pulse had a duration of 30  $\mu\text{sec}$  (to cover the peaking of the pulses from the Čerenkov detector) and a magnitude that exceeded the negative cutoff bias on the CRT. All pulses from the Čerenkov detector were applied to the deflection plates but visible traces appeared only when an intensification signal was applied to the grids of the CRT.

(c) Guard and shower circuits. The pulses from the

<sup>11</sup> Method of measurement is that used by L. H. Meredith, M.S. thesis, State University of Iowa, 1951 (unpublished).

<sup>12</sup> W. C. Elmore and M. Sands, Electronics (McGraw-Hill Book Company, Inc., New York, 1949), p. 58.

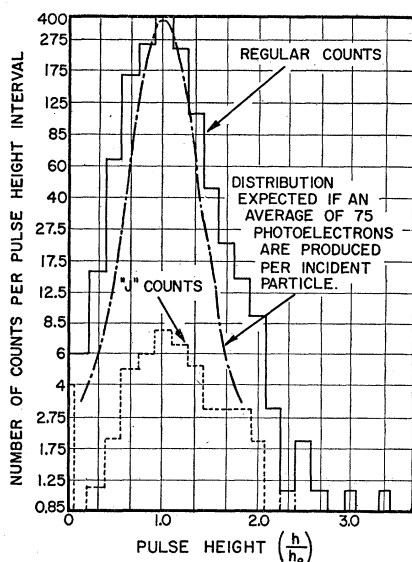


FIG. 4. Differential pulse-height distribution for sea-level  $\mu$  mesons.

guard and shower circuits were placed on the deflection plates at right angles to those used for the pulses of the Čerenkov detector. These pulses were lengthened and shaped in such a way that their peak amplitude occurred at approximately the same time that the gating pulses had driven the grids of the CRT to a point that would just make the trace visible. The traces thus had the appearance of an inverted J. Thus the guard and shower circuits identified as "J" counts all particles passing through the counter telescope accompanied by a particle passing through any of the guard or shower counters. Any count not so marked is termed a "regular" count.

A continuous record of events was made by photographing the traces that appeared on the CRT. The camera shutter was always open and the 35-mm film moved past the lens continuously at the rate of 6 feet per hour.

The entire apparatus was enclosed in a pressure tight aluminum gondola. The total weight of the apparatus when ready for flight was 95 pounds.

### III. SEA LEVEL RESULTS AND INTERPRETATION

In addition to the high-altitude balloon flight a subsequent series of check runs was made with the equipment at  $\lambda = 52^\circ$  using sea-level  $\mu$  mesons as the source of high-energy particles. The identical apparatus that was flown was used for the sea level tests. The purpose of these  $\mu$ -mesons runs was twofold: (1) to analyze and compare the singly charged pulse-height distribution at sea level with those obtained for singly and doubly charged particles at high altitude; and (2) to analyze more carefully certain components in the "J" distribution.

To accomplish the first purpose, the apparatus was run at sea level for a period of 16 hours. The pulse-

height distribution obtained for the 1422 regular counts and 48 "J" counts is shown in Fig. 4. The main features of the pulse-height distribution obtained during this sea level run are explained below.

#### A. Regular Counts

(1) *Half-width of the pulse-height distribution.*—(The term "half-width" is used for the width at half-height, divided by the magnitude of the pulse height at the maximum of the distribution.) The pulse-height distribution for  $\mu$  mesons had a half-width of approximately 48%. One of the major contributing factors to this spread in pulse height is believed to be statistical fluctuations in the output of the photomultiplier. It is well known that the production of photoelectrons at the cathode surface of the photomultiplier and the secondary emission of electrons at each succeeding dynode surface both appear to follow a Poisson distribution.<sup>13</sup>

If these processes are indeed the major cause for spread of the singly charged distributions the half-widths of the pulse height distributions for other particles should vary as  $1/Z$  of the particle. Thus one should expect the distributions to become progressively sharper for higher  $Z$  and to depend more and more on minor effects that contribute to the broadening of the pulse height distributions.

(2) *High-energy tail.*—Another important feature of the pulse height distribution for  $\mu$  mesons is the tail at large pulse heights. This tail is attributed to knock-on electrons of energy greater than the Čerenkov threshold produced by the incident primary particle as it passes through the Lucite block. The additional Čerenkov photons from knock-ons increase the pulse height by varying amounts. This problem of shift in pulse height has been examined for an incident distribution of relativistic singly charged particles by one of the authors.<sup>14</sup> Since the  $\beta$  of the incident particles is assumed

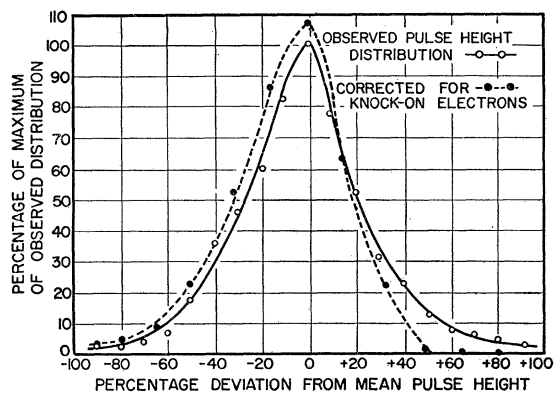


FIG. 5. Effect of knock-on electrons on a typical pulse-height distribution (sea-level  $\mu$ -meson distribution as base).

<sup>13</sup> G. A. Morton, RCA Rev. 10, No. 4, 525 (1949).

<sup>14</sup> W. Webber, M.S. thesis, State University of Iowa, 1955 (unpublished).

to be a constant  $\sim 1$ , both the production of knock-ons and the production of Čerenkov photons vary as  $Z^2$  of the incident particle. Hence, the *relative* shift should be the same for all primaries—regardless of their charge.

The results of this analysis for a typical pulse-height distribution are shown in Fig. 5. The contributions to the pulse-height distribution from knock-on produced photons can be summarized as follows:

(a) The distribution is shifted slightly toward the region of larger pulse heights; (b) the distribution is broadened somewhat, with the half-width being increased approximately 2–3%; (c) a significant tail is added to the distribution in the region of larger pulse heights.

### B. "J" Counts

Before discussing in detail the significance of the "J" counts obtained in the sea-level tests let us consider the types of events that would cause this type of count.

(1) *Accidental coincidences between counter circuits.*—It is possible for a "J" count (or a regular count) to be recorded when two or more unrelated events occur more or less simultaneously in different sets of counters. Such a count will be called an accidental count.

It can be verified that the principal cause of accidental counts is accidental coincidences between the bottom and top telescope trays. Calculations show that the accidental rate from this type of coincidence will vary from about 0.3% of the total counting rate at sea level to approximately 3% at maximum altitude. It is to be expected that these counts are not associated with particles passing through the Lucite block in the prescribed manner (if at all). Therefore their pulse height distribution should show little or no structure.

(2) *Showers and interactions occurring above and to the side of the telescope.*—Although the magnitude of the effect of this type of event on the "J" distribution is difficult to evaluate, it seems reasonable to assume, as before, that such counts are not associated with single particles passing through the Lucite block in the prescribed manner. Therefore, their pulse-height distribution should show little or no structure.

(3) *Knock-on electrons created in the Čerenkov detector.*—It is to be expected that a significant percentage of the knock-on electrons produced by primary particles in the Lucite block and adjacent photomultiplier

TABLE I. Percent of total number of particles of a given charge accompanied by a knock-on electron producing a "J" count.

| Particle           | Charge, $Z$ | Percent of total counts accompanied by a knock-on electron producing a "J" count |
|--------------------|-------------|--|
| ( $p, \mu$ mesons) | 1           | 1.5–2.5  |
| (He)               | 2           | 6.0–10.0   |
| (Li, Be, B)        | Av 4        | 24–32  |
| (C, N, O)          | Av 7        | 50–70  |

TABLE II. Percent of the components of the cosmic radiation that would be expected to have interactions in the counter telescope.

|                 | Thickness             | Protons              |          | Alphas               |          |
|-----------------|-----------------------|----------------------|----------|----------------------|----------|
|                 |                       | M.F.P. <sup>a</sup>  | Per-cent | M.F.P.               | Per-cent |
| Lucite block    | 3.0 g/cm <sup>2</sup> | 63 g/cm <sup>2</sup> | 5.1      | 50 g/cm <sup>2</sup> | 6.1      |
| Photomultiplier | 3.6                   |                      | 5.8      |                      | 7.0      |

<sup>a</sup> Values for M.F.P. (mean free path) are estimated from the results of B. Peters and M. F. Kaplon on similar materials as reported in *Progress in Cosmic Ray Physics*, edited by J. G. Wilson (North Holland Publishing Company, Amsterdam, 1952), p. 209.

will be able to penetrate the guard and shower counters below the block. These knock-ons will cause a "J" count when actually a single primary particle passed through the apparatus. In contrast to the above types of events the pulse-height distribution from this type of event should show definite structure. To find the percentage of particles accompanied by knock-on induced "J" counts one must calculate the number and energy distribution of knock-ons emerging from the Lucite block and the photomultiplier. This problem has been investigated in conjunction with the calculations leading to the effect of the knock-ons on the basic pulse height distribution mentioned in the previous section. The results are summarized in Table I. Note that for heavier particles, the percentage of the total counts that will be recorded as "J's" due to knock-on electrons increases quite rapidly.

It can be seen that this effect becomes an increasing problem with increasing  $Z$ . But since the pulse-height distributions for these counts were found to have structure, it was possible to determine which "J" counts were due to knock-on electrons and then to add these to the pulse height distributions for regular counts.

(4) *Nuclear interactions in the Čerenkov detector.*—These can be grouped into two categories.

(a) Collisions occurring in the Lucite block. The counts due to this type of collision should show little structure in their pulse-height distribution. This is because a nuclear interaction may increase or decrease the output pulse considerably depending on the position of the collision, on the charge and break-up of the primary and on the multiplicity and velocity of the secondaries.

(b) Collisions occurring in the remaining material of the telescope (principally the photomultiplier tube). The pulse height distribution from this type of event should show a definite structure since the primary particle has already passed through the Lucite radiator. The magnitude of the above effects is shown in Table II.

Let us now compare the observed "J" distribution from sea-level  $\mu$  mesons with that predicted in the foregoing sections. Since all other effects are small, the "J" counts in these tests should be due almost entirely to knock-on electrons. To analyze more carefully certain features of this sea level "J" distribution two additional runs were made. In the first of these runs the top guard

TABLE III. Observed "J" distribution from sea-level mesons.

| Run No.                           | Regular counts | "J" counts | Percent "J" counts |
|-----------------------------------|----------------|------------|--------------------|
| No. 1                             | 668            | 18         | $2.6 \pm 0.6$      |
| No. 2                             | 645            | 3          | $0.4 \pm 0.2$      |
| Normal sea level $\mu$ -meson run | 1422           | 48         | $3.3 \pm 0.4$      |

and shower circuits were made inactive, leaving only the bottom guard and shower circuits still functioning. In the second run this procedure was reversed and the top guard and shower circuits now were the only active ones. The results of these runs are shown in Table III.

These results are in good agreement with the predicted results for knock-on electrons. In addition, the pulse height distributions of the "J" counts obtained in the main sea level test and the first special run (bottom guard and shower circuits operating) were similar to that for the regular counts (i.e., had structure)—as would be expected, if these "J" counts were due to knock-on electrons.

#### IV. HIGH-ALTITUDE RESULTS AND INTERPRETATION

##### A. Balloon Flights

The equipment was flown by Winzen Research, Inc., under a contract with the Office of Naval Research, at Goodfellow Air Force Base, San Angelo, Texas ( $41.5^\circ$  N. Geomagnetic latitude) on February 12, 1954. The flight was made using a 90-foot "Skyhook" type balloon to carry the equipment to altitude. The balloon rose at an average rate of 900 ft/min to an altitude of 96 000 ft ( $13.0 \text{ g/cm}^2$ ). It stayed at this altitude,  $\pm 2000$  ft ( $1.0 \text{ g/cm}^2$ ), for a period of six hours. A preset device then cut the equipment loose and it parachuted to earth. The apparatus was recovered near Lampasas, Texas approximately 125 miles from the launching

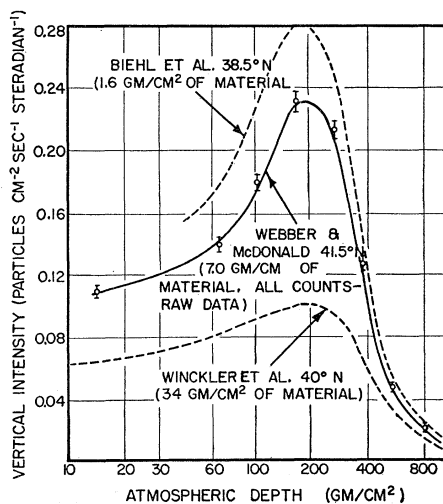


Fig. 6. Vertical intensity of all telescope counts as a function of altitude.

point, having spent the entire period at high altitude at  $41 \pm 0.5^\circ$  N geomagnetic latitude. It was undamaged and still in satisfactory operating condition when returned to the base some 12 hours later.

##### B. Results as a Function of Altitude

The vertical intensity of all telescope counts as a function of altitude is shown in Fig. 6. The time-altitude curve was supplied by Winzen Research, Inc. For comparison, two other sets of results from vertical telescopes, at approximately the same latitude, are shown.

In addition to this over-all examination of the data obtained as the equipment rose to altitude, careful scrutiny was given to the pulse height region from  $h=2.6$  to  $h=5.3$  times the singly charged peak. It was in this region that almost all the Čerenkov pulses from primary alpha particles would be expected. At a depth of approximately  $150 \text{ g/cm}^2$  ( $\sim 3$  mean free paths for

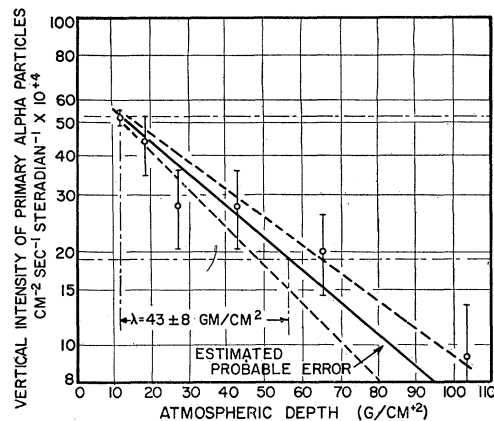


Fig. 7. Vertical intensity of primary alpha particles as a function of altitude (uncorrected), including calculated attenuation M.F.P. in air for these particles.

alpha particles in air) the first regular counts began to appear in this region. The rate at which these counts appeared increased monotonically with altitude up to the highest altitude reached (Fig. 7).

The belief that the particles being counted are true primary alpha particles is thus substantiated by the following facts. (1) The Čerenkov pulses from the particles fall in the region expected for primary alpha particles and; (2) the rate of occurrence of such pulses decreased approximately exponentially with increasing atmospheric depth with a mean free path approximately that expected for alpha particles in air.

##### C. Results at Maximum Altitude

During the two hours operating time at maximum altitude a total of 8213 counts were obtained. The pulse height distribution of the regular counts is shown in Fig. 8. The peak at the position of four times that for relativistic singly charged particles is clearly visible. (Peak to valley ratio 2.8/1.) The pulse-height distribution for the "J" counts is shown in Fig. 9.

If all the pulses lying in the pulse-height region  $0.2 \leq h \leq 2.0$  times the peak of the singly charged particles ( $h_0$ ) are attributed to particles with  $Z=1$ , then those from  $2.6h_0 \leq h \leq 5.3h_0$  correspond to particles with  $Z=2$ ; those from  $7.5h_0 \leq h \leq 24.0h_0$ , to particles with  $3 \leq Z \leq 5$ ; and those above  $24.0h_0$  to particles with  $Z \geq 6$ . On this basis the number of counts, both regular and "J", that can be attributed to each type particle or group of particles is shown in Table IV.

The corrections to the above values that are necessary before one can extrapolate to the top of the atmosphere to obtain absolute primary intensity values will be discussed in the following sections.

**D. Interpretation of Results at Maximum Altitude**

(1) *Singly charged particles.*—It will be noted from Fig. 10 that the half-width of the singly charged dis-

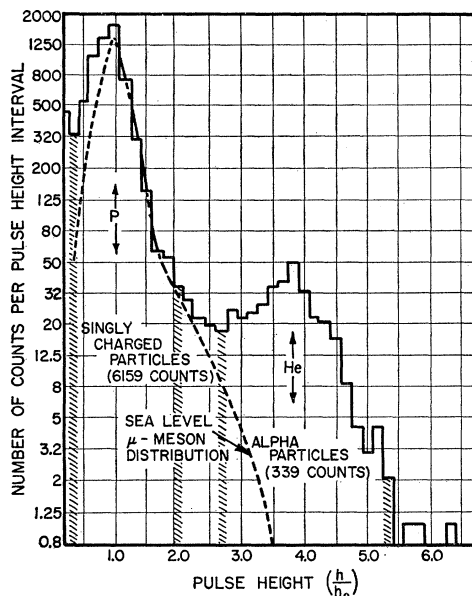


FIG. 8. Pulse-height distribution of regular counts obtained at maximum altitude (note logarithmic scale of ordinate).

tribution at altitude is  $56 \pm 3\%$ , a value greater than that for  $\mu$  mesons at sea level. This result is contrary to what would be expected if the singly charged distribution at high altitude was due entirely to primary protons.

Further comparison of the singly charged pulse-height distribution at high altitude with the sea-level  $\mu$ -meson distribution also indicates that comparatively low energy singly charged particles are filling in the small pulse height region of the singly charged distribution at high altitudes. Notice that this group of secondaries has no effect on the alpha-particle region since their pulses are small. Had this been an instrument that measured ionization loss of these particles, however,

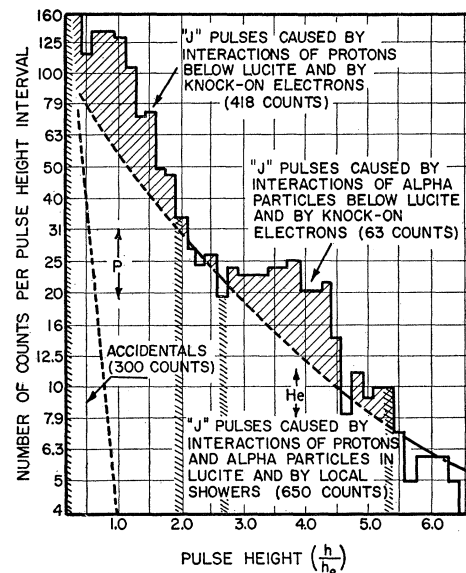


FIG. 9. Pulse-height distribution of "J" counts obtained at maximum altitude. (Note logarithmic scale of ordinate.)

they would have given pulses on the other side of the proton peak and the effect would have been damaging.

To get a rough estimate of the effect of these secondaries on the singly charged distribution assume that all of the counts in the region  $1.2h_0 \leq h \leq 2.0h_0$  of this distribution are due to primary protons. Now since the general shape of the  $\mu$ -meson distribution at sea level very closely approximates the shape of the primary proton distribution that would be expected at maximum altitude, let us normalize the two distributions in the large pulse-height region ( $1.2h_0 \leq h \leq 2.0h_0$ ) and superimpose the  $\mu$ -meson distribution on the singly charged distribution obtained at high altitude. The results are shown in Fig. 10. It is evident from the figure that there is a considerable excess in the low and medium pulse-height regions of the singly charged distribution at altitude over what would be expected if all counts in this distribution were due to primary protons. It is this excess of counts that is believed to be due to singly charged secondary particles.

It should be remarked that the above fitting process is unable to eliminate those secondary particles with  $\beta \sim 1$ . Hence this process should serve only to set a crude upper limit on the intensity of primary protons at this altitude.

TABLE IV. Raw data obtained at 13 g/cm<sup>2</sup> grouped according to apparent Z.

| Charge    | Regular counts | "J" counts |
|-----------|----------------|------------|
| Z=1       | 6159           | 1082       |
| Z=2       | 339            | 298        |
| 3 ≤ Z ≤ 5 | 8              | 63         |
| Z ≥ 6     | 13             | 57         |
| Total     | 6519           | 1500       |

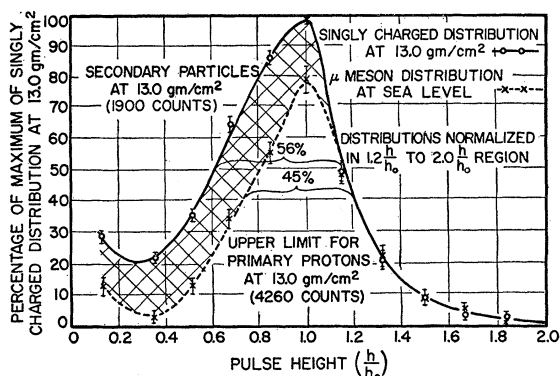


Fig. 10. Sea level  $\mu$ -meson distribution superimposed on the singly charged distribution obtained at 13 g/cm<sup>2</sup> (normalized in region  $1.2h_0 \leq h \leq 2.0h_0$ ).

To find the maximum number of counts attributable to primary protons at 13 g/cm<sup>2</sup> recall that 6159 regular counts were observed in the pulse-height region  $0.2h_0 \leq h \leq 2.0h_0$ . From this we must subtract 1897 counts as being secondaries. According to the previous discussion between 1.5%–2.5% of the total number of protons can be expected to be accompanied by “J” producing knock-on electrons and an additional 6.0% will have collisions in the material below the Lucite block that can cause “J” counts. Thus one would expect 7.5%–8.5% of the proton counts to be accompanied by “J” counts. These counts should show a definite pulse height structure. The interpretation of Fig. 9 shows approximately 418 counts or 8.7% of the total number of proton counts can be attributed to these effects. We must now add to the remaining regular counts these 418 counts that were originally recorded as “J” counts but were actually so labeled due to knock-on electrons and nuclear interactions occurring below the block. Finally, we must take into account the tail of the singly charged (proton) distribution lying above a pulse height  $2.0h_0$  and blending in with alpha-particle distribution (Fig. 11). This accounts for an additional 102 counts. Thus there is a maximum of 4782 counts that can be attributed to primary protons. This gives a vertical intensity of

$$718 \text{ protons/m}^2\text{-steradian-sec at } 41.5^\circ\text{N} \\ \text{at a depth of } 15.5 \text{ g/cm}^2.$$

Note that this is an upper limit for the primary proton intensity at this altitude and may include a considerable fraction of singly charged secondaries with  $\beta \sim 1$ ; therefore it is difficult to assign a meaningful “error” to this result.

(2) *Alpha particles.*—The half-width of the alpha-particle pulse-height distribution is  $30 \pm 6\%$ . This is roughly what would be expected if the principal cause of the half-widths of the various distributions was the statistical production of photoelectrons in the photomultiplier.

In order to obtain an accurate evaluation of the

total number of counts that can be attributed to primary alpha particle we note two important features of the regular pulse-height distribution in the region,  $2.5h_0 \leq h \leq 6.0h_0$ . (a) The valley between the two distributions does not drop to zero, but is approximately 40% of the alpha-particle peak, showing that some type of background exists in this region. (b) The alpha-particle pulse-height distribution appears to drop off quite rapidly to zero except for a possible knock-on electron tail in the region  $4.0h_0 \leq h \leq 6.0h_0$ . This fact shows that the background is quite small in this region.

There are two causes of background in the region between the two distributions. One is the overlapping of the two adjacent distributions. The other is the possibility that the guard and shower devices were not 100% effective in detecting nonalpha events. To estimate the background in the alpha-particle region due to this second cause let us first compare the number of regular counts and “J” counts in the pulse-height region  $6.0h_0 \leq h \leq 8.0h_0$ . Nearly all of the counts in this region should be “J” counts since this region is between the alpha particle and lithium distributions. If a significant number of regular counts occur in this region it would indicate that the guard and shower detection systems were not 100% effective. In this pulse height region 65 “J” counts and only 2 regular counts are obtained, thus we conclude that the detection system is very nearly 100% effective (for “J” counts of this size at least). This deduction is corroborated by the data obtained as the apparatus rose to altitude. All of the 10 pulses with  $h \geq 2.8h_0$  were “J” pulses in the altitude range below 200 g/cm<sup>2</sup> where the heavy primaries  $Z \geq 2$  would not be expected to penetrate.

It thus appears that the principal cause of background between the singly charged distribution and the alpha-particle distribution is the overlapping of the two distributions. This background does not extend throughout the alpha region but contributes only to the low pulse-height side of the alpha peak. This singly charged

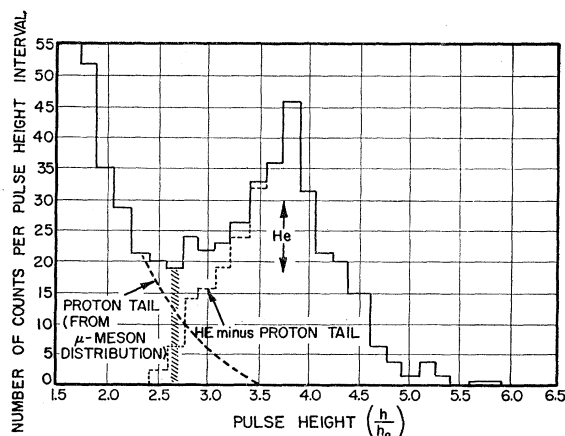


Fig. 11. Enlarged graph of alpha-particle distribution showing the interpolation between the proton and alpha-particle distributions.

(proton) tail can be subtracted with accuracy, since whether this tail is due to knock-on electrons or statistical fluctuations, or both, it should have the same shape as the known  $\mu$ -meson tail. Therefore after proper normalization we may simply subtract out the tail obtained from the sea level runs on  $\mu$  mesons. This is done in Fig. 11. The subtraction removes a total of 28 counts that we originally attributed to alpha particles. According to the previous calculations 6–10% of the total number of alpha particles will be accompanied by “J” producing knock-ons, and an additional 7% will be accompanied by “J” counts caused by collisions. Thus one would expect 13–17% of the total number of alpha particles to be accompanied by “J” counts. Examination of the “J” pulse-height distribution in Fig. 9 in the region  $2.0h_0 \leq h \leq 6.0h_0$  shows that approximately 63 counts or 16.5% of the total number of alpha particle counts can be attributed to these effects. These 63 “J” counts that were so labeled due to knock-on electrons and nuclear interactions occurring below the block must now be added to the counts that were originally attributed to alpha particles.

The total number of counts that can finally be attributed to primary alpha particles is thus 374. Extrapolating to the top of the atmosphere from the bottom of the Lucite radiator (13.0 g/cm<sup>2</sup> of air + 2.5 g/cm<sup>2</sup> of local material) using a M.F.P. of 445 g/cm<sup>2</sup> (see reference a of Table II) gives for the vertical intensity of primary alpha particles:

$$82 \pm 9 \text{ (m}^2 \text{ steradian sec)}^{-1} \text{ at } 41.5^\circ \text{ N}$$

with all statistical and experimental errors included.

(3) *Particles with  $Z > 2$ .*—Any attempt to obtain an accurate value for the intensity of these heavier particles is complicated by the following factors: (a) The statistics obtained were poor; (b) no resolved pulse-height distributions were obtained; (c) the correction for knock-on electrons and nuclear interactions occurring below the block and thus causing “J” counts became larger and progressively more uncertain for the larger values of  $Z$ . Nevertheless it is illuminating to get a rough measure of the intensities of this component as measured by this type of detector.

Using (a) the  $Z^2$  dependence of Čerenkov light and (b) the amplifier calibration curves, a total of 8 regular counts were obtained in the  $3 \leq Z \leq 5$  ( $L$ ) region and a total of 13 regular counts in the  $Z \geq 6$  ( $M+H$ )

region. Making corrections for “J” counts caused by knock-on electrons and for nuclear interactions below the block gives a total of  $11 \pm 5$  ( $L$ ) counts and  $35 \pm 15$  ( $M+H$ ) counts. These values correspond to vertical intensities of 1.6 and 5.1 particles/m<sup>2</sup> steradian sec, respectively, at a depth of 15.5 g/cm<sup>2</sup>. The  $L/(M+H)$  ratio at this depth is thus  $0.31 \pm 0.2$ . It is to be emphasized that these are very rough values. They are given only for the sake of completeness.

## V. COMPARISON WITH PREVIOUS MEASUREMENTS OF THE ALPHA-PARTICLE INTENSITY AT 41°N

In conclusion, the experimental results of many observers using various techniques are summarized in Table V for the alpha-particle intensity at 41°N.

TABLE V. Comparison of vertical primary alpha-particle intensities obtained at the top of the atmosphere by different experimenters ( $\lambda \sim 41^\circ \text{N}$ ).

| Author               | Reference | Method                             | Lat.  | Alpha-particle intensity (particles/m <sup>2</sup> steradian-sec) |
|----------------------|-----------|------------------------------------|-------|---|
| Webber<br>McDonald   | —         | Čerenkov detector                  | 41.5° | 82 ± 9  |
| Bohl                 | 5         | Double scintillator                | 41.5° | 90 ± 8  |
| Linsley              | 10        | Čerenkov detector and cloud chamb. | 41.5° | 92 ± 15   |
| Horowitz             | 9         | Čerenkov detector                  | 41.5° | 99 ± 15   |
| Perlow <i>et al.</i> | 3         | Proportional counters              | 40.0° | 110 ± 20  |
| Bradt and Peters     | 6         | Photographic emulsions             | 41.7° | 138 ± 20  |

It is noteworthy that the most recent values lie markedly below the earlier ones.<sup>3,6</sup> This tendency in the data is believed due to progressively better resolution and identification of alpha particles.

## VI. ACKNOWLEDGMENTS

The authors wish to express their sincere thanks to Professor J. A. Van Allen who not only provided the opportunity to conduct this research but made many valuable suggestions throughout the analysis of the data.

Special notes of thanks are also due to G. H. Ludwig and to J. G. Sentinella and other members of the shop, for construction of the equipment.

The equipment was carried aloft by “Skyhook” balloons supplied by Winzen Research, Inc.